$pp \to pp\pi^0$ near threshold in pionless effective field theory

Shung-ichi Ando*
Department of Physics, Sungkyunkwan University, Suwon 440-746, Korea

In this talk, we review our recent calculation for the $pp \to pp\pi^0$ reaction near threshold in pionless effective field theory with a di-baryon and external pions.

PACS numbers: 13.60.Le, 25.10.+s.
Keywords: $pp \to pp\pi^0$, pionless effective field theory

I. INTRODUCTION

The study of neutral pion production in proton-proton collision near threshold, $pp \to pp\pi^0$, has been inspired by precise measurements of the near-threshold cross section[1,2]. Surprisingly, the measured cross section turned out to be ~ 5 times larger than the early theoretical predictions[3]. Subsequently, some mechanisms to account for the threshold experimental data have been suggested in model calculations[4].

Heavy-baryon chiral perturbation theory (HBχPT) is a low-energy effective field theory (EFT) of QCD and provides us a systematic perturbation scheme in terms of Q/Λ_χ where Q denotes small external momentum and/or symmetry breaking term m_π and Λ_χ denotes the chiral scale $\Lambda_\chi = 4\pi f_\pi \simeq 1$ GeV: f_π is the pion decay constant. Though many works on the $pp \to pp\pi^0$ reaction near threshold in HBχPT have been done[5,6,7,8,9,10,11,12] (for a recent review, see Ref.[13] and references therein), some issues in theoretically describing the process have not been fully clarified. In the next-to-leading order (NLO) HBχPT calculations[5,6,7], a significant enhancement of the off-shell $\pi\pi NN$ vertex function obtained from the NLO HBχPT Lagrangian is found. However, the two-body (one-pion-exchange) matrix element with the off-shell $\pi\pi NN$ vertex is almost exactly canceled with the one-body matrix element. Thus the experimental data cannot be reproduced in the NLO calculations. In the next-to-next-to leading order (NNLO) HBχPT calculations[8,9,10], a significant contribution comes out of the NNLO corrections and a moderate agreement with the experimental data is obtained[9]. However, the chiral series based on the standard Weinberg's counting rules[14] shows poor convergence.

A modification of the original Weinberg's counting rules to account for the large momentum transfer, $k \simeq \sqrt{m_\pi m_N}$ where m_π and m_N are the pion and nucleon masses, respectively, is discussed in Ref.[6]. The production operators at NLO using the modified counting rules are estimated, and it was reported that the NLO contributions exactly cancel among themselves[15]. Recently, some detailed issues for the loop calculations, such as a concept of reducibility[16], a representation invariance of the chiral fields among the loop diagrams, and a proper choice of the heavy-nucleon propagator[17], were also studied.

Meanwhile, it is known that the energy dependence of the experimental data can be well reproduced in terms of the final state interaction and the phase space[2]. A "minimal" formalism to take account of these two features would be a *pionless* theory, in which virtual pions exchanged between the two nucleons are integrated out; in this pionless theory, the one-pion exchange, two-pion exchange and contact terms in HBχPT are subsumed in a contact term. Furthermore, after taking these two features into account, the difference between the theory and experiment appears in the overall factor and the experimental data can be easily reproduced by fitting an unknown constant that appears in a contact vertex. In this work[18] we employ a pionless EFT with a di-baryon[19,2030] and external pions[23] to calculate the total cross section of the $pp \to pp\pi^0$ process.

II. PIONLESS EFFECTIVE LAGRANGIAN

An effective Lagrangian without virtual pions and with a di-baryon and external pions for describing the $pp \to pp\pi^0$ reaction may read

$$\mathcal{L} = \mathcal{L}_N + \mathcal{L}_s + \mathcal{L}_{Ns\pi} + \mathcal{L}^P_{NN}\,, \tag{1}$$

where $\mathcal{L}_N$ is the standard one-nucleon Lagrangian in heavy-baryon formalism where the "external" pions are nonlinearly realized. $\mathcal{L}_s$ is for the ${}^1S_0$ channel di-baryon field, $\mathcal{L}_{Ns\pi}$ represents the contact interaction of an external pion, a di-baryon and two nucleons, and $\mathcal{L}^P_{NN}$ is for the two-nucleon ${}^3P_0$ channel. The effective Lagrangian for the two-nucleon part may read[19,20,24,25]

$$\begin{aligned}
\mathcal{L}_s &= \sigma_s s_a^\dagger \left[iv\cdot D + \frac{1}{4m_N}[(v\cdot D)^2 - D^2] + \delta_s \right] s_a \\
&\quad - y_s \left[s_a^\dagger (N^T P_a^{({}^1S_0)} N) + \text{h.c.} \right], \qquad (2)\\
\mathcal{L}_{Ns\pi} &= \frac{\tilde{d}_\pi^{(2)}}{\sqrt{8m_N r_0}} \left\{ i\epsilon_{abc} s_a^\dagger \left[N^T \sigma_2 \vec{\sigma}\cdot i(\overrightarrow{D} - \overleftarrow{D}) \tau_2 \tau_b N \right] \right. \\
&\quad \left. \times (iv\cdot\Delta_c) + \text{h.c.} \right\}, \qquad (3)\\
\mathcal{L}^P_{NN} &= C_2^0 \delta_{ij}\delta_{kl} \frac{1}{4} \left(N^T \mathcal{O}^{1,P}_{ij,a} N \right)^\dagger \left(N^T \mathcal{O}^{1,P}_{kl,a} N \right) + \cdots \qquad (4)
\end{aligned}$$

with $\mathcal{O}^{1,P}_{ij,a} = i(\overleftarrow{D}_i \;\; P^{(P)}_{j,a} - P^{(P)}_{j,a} \;\; \overrightarrow{D}_i)$ and $P^{(P)}_{i,a} = \frac{1}{\sqrt{8}}\sigma_2\sigma_i\tau_2\tau_a$. s_a is the ${}^1S_0$ channel di-baryon field and σ_s is the sign factor $\sigma_s = \pm 1$ which we fix below. v^μ is a

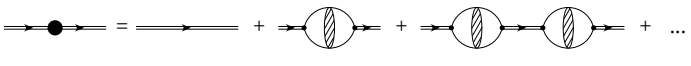

FIG. 1: Diagrams for the dressed di-baryon propagator including the Coulomb interaction.

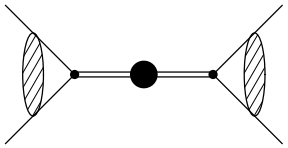

FIG. 2: Diagram for the S-wave pp scattering amplitude with the Coulomb interaction.

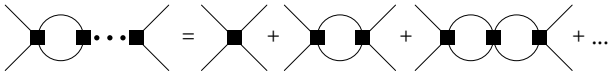

FIG. 3: Diagrams for the P-wave NN scattering.

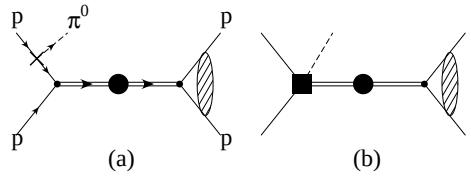

FIG. 4: Diagrams for $pp \to pp\pi^0$ near threshold with the strong and Coulomb final state interactions and without the initial state interaction.

velocity vector $v^\mu = (1, \vec{0})$ and D_μ is the covariant derivative. δ_s is the mass difference between the di-baryon mass m_s and two-nucleon mass, $m_s = 2m_N + \delta_s$. y_s is the coupling constant of the di-baryon and two-nucleon interaction. $P_i^{(^1S_0)} = \frac{1}{\sqrt{8}}\tau_2\tau_a\sigma_2$. $d_\pi^{(2)}$ is an unknown low energy constant (LEC) of the (external) pion-(spin singlet) dibaryon-nucleon-nucleon (πsNN) interaction. r_0 is the effective range in the $^1S_0$ (pp) channel, and $\Delta^\mu = \frac{\tau_a}{2}\Delta_a^\mu$. C_2^0 is the LEC for the NN scattering in the $^3P_0$ channel.

Now we calculate the S- and P-wave NN scattering amplitudes to fix the LECs in the two-nucleon part. In Fig. 1, diagrams for the dressed $^1S_0$ channel di-baryon propagator are shown where the two-nucleon bubble diagrams including the Coulomb interaction are summed up to the infinite order. In Fig. 2, a diagram of the S-wave pp scattering amplitude with the Coulomb interaction is shown and thus we have the S-wave scattering amplitude as

$$\begin{aligned} i\mathcal{A}_s &= (-iy_s\psi_0)\,[iD_s(p)]\,(-iy_s\psi_0) \\ &= i\frac{4\pi}{m_N}\frac{C_\eta^2 e^{2i\sigma_0}}{-\frac{4\pi\sigma_s\delta_s^R}{m_N y_s^2} - \frac{4\pi\sigma_s p^2}{m_N^2 y_s^2} - \alpha m_N h(\eta) - ip\,C_\eta^2}\,, \end{aligned} \tag{5}$$

where $\psi_0 = C_\eta e^{i\sigma_0}$ and σ_0 is the S-wave Coulomb phase shift $\sigma_0 = \arg\Gamma(1+i\eta)$. $D_s(p)$ is the dressed di-baryon propagator and δ_s^R is the renormalized mass difference. $h(\eta) = Re\,\psi(i\eta) - \ln\eta$, $Re\,\psi(\eta) = \eta^2\sum_{\nu=1}^{\infty}\frac{1}{\nu(\nu^2+\eta^2)} - \gamma$, $\gamma = 0.5772\cdots$, and

$$C_\eta^2 = \frac{2\pi\eta}{e^{2\pi\eta}-1}\,, \quad \eta = \frac{\alpha m_N}{2p}\,. \tag{6}$$

The S-wave amplitude $\mathcal{A}_s$ is given in terms of the effective range parameters as

$$i\mathcal{A}_s = i\frac{4\pi}{m_N}\frac{C_\eta^2 e^{2i\sigma_0}}{-\frac{1}{a_C} + \frac{1}{2}r_0p^2 + \cdots - \alpha m_N h(\eta) - ip\,C_\eta^2}\,, \tag{7}$$

where a_C is the scattering length, r_0 is the effective range, and the ellipsis represents the higher order corrections. Now it is easy to match the LECs with the effective range parameters. Thus we have $\sigma_s = -1$ and

$$y_s = \pm\frac{2}{m_N}\sqrt{\frac{2\pi}{r_0}}\,, \tag{8}$$

$$D_s(p) = \frac{m_N r_0}{2}\frac{1}{\frac{1}{a_C} - \frac{1}{2}r_0p^2 + \alpha m_N h(\eta) + ip\,C_\eta^2}\,. \tag{9}$$

We note that the sign of the LEC y_s cannot be determined by the effective range parameters.

In Fig. 3, diagrams for the P-wave NN scattering are shown. Because the momenta of the two protons are quite large for the pion production reaction, the two-proton bubble diagrams are summed up to the infinite order. The scattering amplitude for the $^3P_0$ channel is obtained as

$$i\mathcal{A}_p = \frac{4\pi}{m_N}\frac{ip^2}{\frac{4\pi}{m_N C_2^0} - ip^3}\,. \tag{10}$$

The LEC C_2^0 is fixed by the phase shift of the $^3P_0$ channel at pion production threshold, $\delta_p(p_{th}) \simeq -7.5^\circ$ at $p_{th} \simeq \sqrt{m_\pi m_N}$. Thus we have

$$\frac{4\pi}{m_N C_2^0} \simeq p_{th}^3\cot\delta_p(p_{th})\,. \tag{11}$$

III. AMPLITUDES FOR $pp \to pp\pi^0$ NEAR THRESHOLD

In Figs. 4 and 5, we show diagrams for $pp \to pp\pi^0$ near threshold. In diagram (a) in Fig. 4 and (c) in Fig. 5, the pion is emitted from the one-body πNN vertex. In the diagram (b) in Fig. 4 and (d) in Fig. 5, the pion is emitted from the πsNN contact vertex which is proportional to the LEC $\tilde{d}_\pi^{(2)}$. The one-body amplitude from the (a) and (c) diagrams and the two-body (contact) amplitude from the (b) and (d) diagrams are obtained as

$$i\mathcal{A}_{(a+c)} = -\frac{4\pi g_A}{m_N^2 f_\pi}\frac{1}{1 - \frac{m_N C_2^0}{4\pi}ip^3}$$

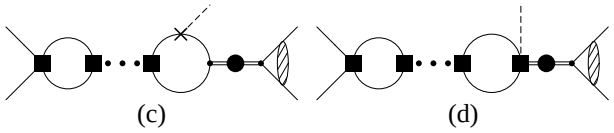

FIG. 5: Diagrams for $pp \to pp\pi^0$ with the strong initial and the strong and Coulomb final state interactions.

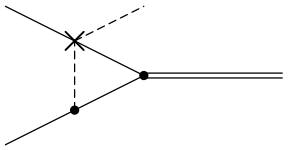

FIG. 6: Diagram for a one-pion exchange contribution to the $pp \to pp\pi^0$ process for estimating the LEC $\tilde{d}_\pi^{(2)}$ in the contact vertex.

$$\times \frac{C_{\eta'} e^{i\sigma_0} p}{\frac{1}{a_C} - \frac{1}{2} r_0 p'^2 + \alpha m_N h(\eta') + ip' C_{\eta'}^2}\,, \qquad (12)$$

$$i\mathcal{A}_{(b+d)} = 4\sqrt{\frac{2\pi}{m_N}} \frac{\tilde{d}_\pi^{(2)}}{f_\pi} \frac{1}{1 - \frac{m_N C_0^2}{4\pi} ip^3} \times \frac{C_{\eta'} e^{i\sigma_0} \omega_q p}{\frac{1}{a_C} - \frac{1}{2} r_0 p'^2 + \alpha m_N h(\eta') + ip' C_{\eta'}^2} \qquad (13)$$

where $2\vec{p}$ and $2\vec{p}'$ are the relative three momenta between incoming and outgoing two protons, respectively; $p = |\vec{p}|$ and $p' = |\vec{p}'|$. $\eta' = \alpha m_N/(2p')$ and ω_q is the energy of outgoing pion, $\omega_q = \sqrt{\vec{q}^2 + m_\pi^2}$: $\vec{q}$ is the outgoing pion momentum. We note that there remain no unknown parameters in the amplitudes except for the LEC $\tilde{d}_\pi^{(2)}$ in the two-body (contact) amplitude in Eq. (13).

Now we estimate an order of magnitude of the LEC $\tilde{d}_\pi^{(2)}$ from HBχPT. We here consider a one-pion-exchange (OPE) diagram shown in Fig. 6. This diagram is the lowest order OPE contribution in the standard Weinberg counting rules. We include a higher order (relativistic) correction to the $\pi\pi NN$ vertex which is found to be important[12] and is, in the modified counting rules, of the same order as the lowest order diagram.

The effective chiral Lagrangian to calculate the isoscalar $\pi\pi NN$ interaction in the diagram in Fig. 6, reads[28] $\mathcal{L}_{\pi N} = \mathcal{L}_{\pi N}^{(2)} + \mathcal{L}_{\pi N}^{(3)} + \cdots$ where

$$\mathcal{L}_{\pi N}^{(2)} = N^\dagger \left[c_1 \mathrm{Tr}(\chi_+) + \left(\frac{g_A^2}{2m_N} - 4c_2 \right) (v\cdot\Delta)^2 - 4c_3 \Delta\cdot\Delta \right] N + \cdots\,, \qquad (14)$$

and $\mathcal{L}_{\pi N}^{(3)}$ is the relativistic correction to the term proportional to $(v\cdot\Delta)^2$ in Eq. (14). The values of the LECs c_1, c_2 and c_3 are fixed in the tree-level calculations[29] as

$$c_1 = -0.64\,, \quad c_2 = 1.79\,, \quad c_3 = -3.90 \ \ [\mathrm{GeV}^{-1}]\,. \qquad (15)$$

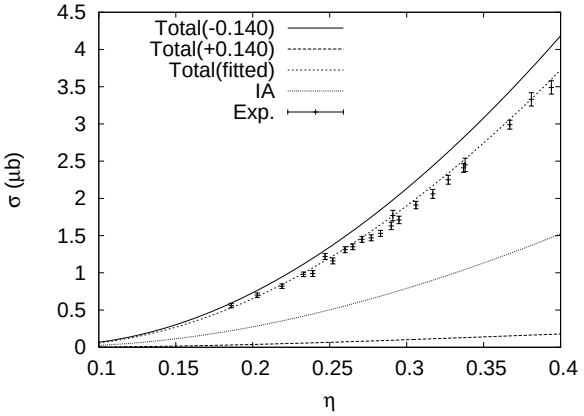

FIG. 7: Estimated total cross section of $pp \to pp\pi^0$ as a function of $\eta_\pi = |\vec{q}|_{max}/m_\pi$. See the text for details.

The value of the LEC $\tilde{d}_\pi^{(2)}$ from the loop diagram in Fig. 6 is obtained as

$$\tilde{d}_\pi^{(2)} \simeq \pm \frac{\sqrt{2\pi} g_A}{32 m_\pi^{3/2}} \frac{m_\pi^2}{f_\pi^2} \left(-4c_1 + 2c_2 - \frac{3g_A^2}{16 m_N} + c_3 \right) \simeq \pm 0.140 \ \ \mathrm{fm}^{5/2}\,, \qquad (16)$$

where the different signs for $\tilde{d}_\pi^{(2)}$ have been obtained because of the LEC y_s in Eq. (8).

IV. NUMERICAL RESULTS AND SUMMARY

The total cross section of $pp \to pp\pi^0$ near threshold is calculated using the formula

$$\sigma = \frac{1}{2} \int_0^{q^{max}} dq \frac{d\sigma}{dq}, \quad \frac{d\sigma}{dq} = \frac{1}{v_{lab}} \frac{m_N q^2 p'}{16(2\pi)^3 \omega_q} \sum_{spin} |\mathcal{A}|^2, \qquad (17)$$

with $p' = |\vec{p}'| \simeq \sqrt{m_N(T - \sqrt{m_\pi^2 + q^2}) - q^2/4}$, and $q^{max} \simeq \sqrt{\frac{T^2 - m_\pi^2}{1 + \frac{T}{2m_N}}}$. T is the initial total energy $T \simeq \vec{p}^2/m_N$ and $v_{lab} \simeq 2p/m_N$. We have expanded the proton energies in the phase factor in terms of $1/m_N$ and kept up to the $1/m_N$ order. $\mathcal{A}$ is the amplitude $\mathcal{A} = \mathcal{A}_{(a+c)} + \mathcal{A}_{(b+d)}$ where $\mathcal{A}_{(a+c)}$ and $\mathcal{A}_{(b+d)}$ are obtained in Eqs. (12) and (13), respectively.

In Fig. 7 we plot our results for the total cross section as a function of $\eta_\pi = q^{max}/m_\pi$. The solid curve and long-dashed curve have been obtained by using $\tilde{d}_\pi^{(2)} = \pm 0.140$ fm$^{5/2}$ fixed from the one-pion exchange diagram in Fig. 6 in the previous section. The LEC $\tilde{d}_\pi^{(2)}$ is also fixed by using the experimental data as

$$\tilde{d}_\pi^{(2)fitted} = -0.12\,, \quad +0.55 \ \mathrm{fm}^{5/2}\,, \qquad (18)$$

where we have two values of $\tilde{d}_\pi^{(2)}$ with different signs. The short-dashed curve is obtained by using $\tilde{d}_\pi^{(2)fitted} =$

-0.12 fm$^{5/2}$. The dotted line corresponds to the case where only the contribution from the one-body amplitude $\mathcal{A}_{(a+c)}$ is considered. The experimental data are also included in the figure.

We find that the experimental data are reproduced reasonably well with the value of $\tilde{d}_\pi^{(2)} = -0.14$ fm$^{5/2}$. By contrast, we obtain almost vanishing total cross sections with the value $\tilde{d}_\pi^{(2)} = +0.140$ fm$^{5/2}$ because the two-body amplitude with $\tilde{d}_\pi^{(2)} = +0.140$ fm$^{5/2}$ is almost canceled with the amplitude from the one-body contribution. On the other hand, for the whole energy range the experimental near-threshold cross section data are well reproduced with the use of the fitted parameter $\tilde{d}_\pi^{(2)fitted} = -0.12$ fm$^{5/2}$. We also find that approximately a half of the observed cross section comes from the one-body (IA) amplitude in the pionless theory.

In this work we calculated the total cross section for $pp \to pp\pi^0$ near threshold in pionless EFT with the dibaryon and external pion fields. The leading one-body amplitude and subleading contact amplitude were obtained including the strong initial state interaction and the strong and Coulomb final-state interactions. After we fix the LECs for the NN scatterings, there remains only one unknown constant, $\tilde{d}_\pi^{(2)}$, in the amplitude. We estimated it from the one-pion exchange diagram in the pionful theory. Although this method does not allow us to fix the sign of $\tilde{d}_\pi^{(2)}$, we have found that one of the two choices for $\tilde{d}_\pi^{(2)}$ leads to the cross sections that agree with the experimental data reasonably well. On the other hand, the whole range of the experimental data near threshold can be reproduced by adjusting the only unknown LEC in the theory, $\tilde{d}_\pi^{(2)}$. As discussed in Introduction, this is an expected result because the energy dependence of the experimental total cross section is known to be well described by the phase factor and the final-state interaction[2], which have been taken into account in this work, and the overall strength of the cross section can be adjusted by the value of $\tilde{d}_\pi^{(2)}$. This feature would be the same in the NNLO HBχPT calculations because an unknown constant appears in the contact $\pi NNNN$ vertex and can be adjusted so as to reproduce the experimental data though there are many other corrections coming out of the pion loop diagrams.

Acknowledgments

The author would like to thank the organizers for the conference APPC10, August 21-24, 2007, Pohang, Korea for hospitality. This work is supported by Korean Research Foundation and The Korean Federation of Science and Technology Societies Grant founded by Korean Government (MOEHRD, Basic Research Promotion Fund): the Brain Pool program (052-1-6) and KRF-2006-311-C00271.

* Electronic address: sando@color.skku.ac.kr

[1] H. O. Meyer *et al.*, Phys. Rev. Lett. **23** (1990) 2846.
[2] H. O. Meyer *et al.*. Nucl. Phys. **A 539** (1992) 633.
[3] D. S. Koltum and A. Reitan, Phys. Rev. **141** (1966) 1413: G. A. Miller and P. U. Sauer, Phys. Rev. C **44** (1991) R1725.
[4] T.-S. H. Lee, D. O. Riska, Phys. Rev. Lett. **70** (1993) 2237: E. Hernández, E. Oset, Phys. Lett. **B 350** (1995) 158.
[5] B.-Y. Park, , F. Myhrer, J. R. Morones, T. Meissner, and K. Kubodera, Phys. Rev. C **53** (1996) 1519.
[6] T. D. Cohen, J. L. Friar, G. A. Miller, and U. van Kolck, Phys. Rev. C **53** (1996) 2661.
[7] T. Sato, T.-S. H. Lee, F. Myhrer, and K. Kubodera, Phys. Rev. C **56** (1997) 1246.
[8] V. Dmitrašinović, K. Kubodera, F. Myhrer, and T. Sato, Phys. Lett. **B 465** (1999) 43.
[9] S. Ando, T.-S. Park, and D.-P. Min, Phys. Lett. **B 509** (2001) 253.
[10] Y. Kim, T. Sato, F. Myhrer, and K. Kubodera, arXiv:0704.1342.
[11] U. van Kolck, G. A. Miller, and D. O. Riska, Phys. Lett. **B 388** (1996) 679.
[12] V. Bernard, N. Kaiser, U.-G. Meißner, Eur. Phys. J. A **4** (1999) 259.
[13] C. Hanhart, Phys. Rep. **397** (2004) 155.
[14] S. Weinberg, Phys. Lett. **B 251** (1990) 288; Nucl. Phys. **B 363** (1991) 3.
[15] C. Hanhart and N. Kaiser, Phys. Rev. C **66** (2002) 054005.
[16] V. Lensky, V. Baru, J. Haidenbauer, C. Hanhart, A. E. Kudrayavtsev, and U.-G. Meißner, Eur. Phys. J. **A 27** (2006) 37.
[17] C. Hanhart and A. Wirzba, Phys. Lett. **B 650** (2007) 354.
[18] S. Ando, arXiv:0707.2157, to appear in Eur. Phys. J. **A**.
[19] S. R. Beane, M. J. Savage, Nucl. Phys. **A 694** (2001) 511.
[20] S. Ando and C. H. Hyun, Phys. Rev. C **72** (2005) 014008.
[21] S. Ando, R. H. Cyburt, S. W. Hong, C. H. Hyun, Phys. Rev. C **74** (2006) 025809.
[22] S. Ando and K. Kubodera, Phys. Lett. **B 633** (2006) 253.
[23] S. R. Beane, M. J. Savage, Nucl. Phys. **A 717** (2003) 104.
[24] J.-W. Chen, G. Rupak, M. J. Savage, Nucl. Phys. **A 653** (1999) 386.
[25] S. Fleming, T. Mehen, I. W. Stewart, Nucl. Phys. **A 677** (2000) 313.
[26] X. Kong and F. Ravndal, Phys. Lett. **B 450** (1999) 320.
[27] S. Ando, J. W. Shin, C. H. Hyun, S. W. Hong, arXiv:0704.2312.
[28] N. Fettes, U.-G. Meißner, M. Mojžiš, S. Steininger, Ann. of Phys. **283** (2000) 273; ibid **288** (2001) 249.
[29] V. Bernard, N. Kaiser, U.-G. Meißner, Nucl. Phys. **B 457** (1995) 147.
[30] We have studied $np \to d\gamma$ cross section at BBN energies[21] and neutron-neutron fusion process[22] employing this formalism.